

Lawrence Berkeley National Laboratory

LBL Publications

Title

Thermal and capillary effects on the caprock mechanical stability at In Salah, Algeria

Permalink

<https://escholarship.org/uc/item/6pv2v2g7>

Journal

Greenhouse Gases Science and Technology, 5(4)

ISSN

2152-3878

Authors

Vilarrasa, Víctor
Rutqvist, Jonny
Rinaldi, Antonio Pio

Publication Date

2015-08-01

DOI

10.1002/ghg.1486

Peer reviewed

**Thermal and capillary effects on the caprock mechanical stability at In Salah,
Algeria**

Víctor Vilarrasa^{1,2}, Jonny Rutqvist¹ and Antonio Pio Rinaldi^{1,3}

¹ Lawrence Berkeley National Laboratory (LBNL), 1 Cyclotron Rd, Berkeley, CA
94720, USA

² Soil Mechanics Laboratory, Swiss Federal Institute of Technology, EPFL, Lausanne
Switzerland

³ Swiss Seismological Service, Swiss Federal Institute of Technology, ETHZ, Zurich
Switzerland

ABSTRACT

Thermo-mechanical effects are important in geologic carbon storage because CO₂ will generally reach the storage formation colder than the rock, inducing thermal stresses. Capillary functions, i.e., retention and relative permeability curves, control the CO₂ plume shape, which may affect overpressure and thus, caprock stability. To analyze these thermal and capillary effects, we numerically solve non-isothermal injection of CO₂ in deformable porous media considering the In Salah, Algeria, CO₂ storage site. We find that changes in the capillary functions have a negligible effect on overpressure and thus, caprock stability is not affected by capillary effects. However, we show that for the strike slip stress regime prevalent at In Salah, stability decreases in the lowest parts of the caprock during injection due to cooling-induced thermal stresses. Simulations show that shear slip along pre-existing fractures may take place in the cooled region, whereas tensile failure is less likely to occur. Indeed, only the injection zone and the lowest tens of meters of the 900 m thick caprock at In Salah might be affected by cooling effects, which would thus not jeopardize the overall sealing capacity of the caprock. Furthermore, faults are likely to remain stable far away from the injection well because outside the cooled region the injection-induced stress changes are not sufficient to exceed the anticipated shear strength of minor faults. Nevertheless, we recommend that thermal effects should be considered in the site characterization and injection design of future CO₂ injection sites to assess caprock stability and guarantee a permanent CO₂ storage.

Keywords: thermal stresses, induced seismicity, geologic carbon storage, geomechanical stability

1. INTRODUCTION

Thermal effects have a significant impact in geologic carbon storage because carbon dioxide (CO₂) will not thermally equilibrate with the geothermal gradient in its way down the injection well, especially at high flow rates¹. Therefore, CO₂ will reach the bottom of the well at a lower temperature than the storage formation. A clear example of this temperature difference can be found at In Salah, Algeria, where, even injecting CO₂ at the wellhead at 35 °C (5 °C warmer than the ambient temperature), CO₂ reached the storage formation at 50 °C, resulting in a temperature difference with the storage formation of 45 °C². Another example is Cranfield, Mississippi, where CO₂ enters the storage formation 44 °C colder than the rock³. Furthermore, CO₂ may be injected in liquid conditions because it significantly reduces the compression costs at the wellhead, which would lead to a significant temperature difference⁴.

The injection of a fluid that is colder than the host rock has already been studied in enhanced geothermal systems⁵⁻⁹. However, only a few studies have dealt with the coupled thermo-hydro-mechanical analysis of cold CO₂ injection^{4, 10-14}. This scarcity of studies is probably due to the high complexity given by the two-phase flow nature of CO₂ injection in saline formations, together with the non-ideality of CO₂. Nevertheless, thermo-mechanical effects are receiving increased attention and thus, an increasing number of research groups are considering this problem.

The necessity of further investigation is evident due to the apparent contradiction between results of some of these thermo-mechanical studies. Though all studies agree that there will be a thermal stress reduction in the reservoir that could induce microseismicity and enhance reservoir permeability, the effects on caprock stability differ. For instance, while the simulations of Preisig and Prevost¹⁰ and Gor et al.¹³

yielded tensile failure in the caprock after some years of injecting cold CO₂, the results of Vilarrasa et al.^{4, 14} showed that the stability in the lower part of the caprock increases around the injection well due to a stress redistribution caused by the thermal stress reduction in the reservoir. These differences may arise from the different geological setting that they investigated. Preisig and Prevost¹⁰ and Gor et al.¹³ based their studies on the geological setting of the In Salah CO₂ storage site, which is a thin reservoir (20 m thick). However, Vilarrasa et al.^{4, 14} considered a 100 m thick reservoir in both normal and reverse faulting stress regimes. The relevance of the stress state on the thermo-mechanical response is highlighted by the variation in the results of Preisig and Prevost¹⁰ and Gor et al.¹³. Even though they considered the same geometry and geomechanical properties, Preisig and Prevost¹⁰ results yielded tensile failure after 3 years of injection by assuming a hypothetical normal faulting stress regime, but Gor et al.¹³ results predicted tensile failure after 12 years of injection using the actual strike slip stress regime of the site. Another aspect that may have an influence in the results of Preisig and Prevost¹⁰ and Gor et al.¹³ is the fact that they do not simulate the basement rock below the injection zone. Therefore, the bottom of the reservoir is a no flow boundary that does not allow temperature to dissipate into the basement and thus, a higher temperature drop may occur towards the caprock. Hence, a detailed modeling of each injection site will be needed to properly assess thermo-mechanical effects.

The study of a real injection site, like In Salah, can give valuable insight into the relevant thermo-hydro-mechanical processes that occur as a result of CO₂ injection. A real site provides data, such as ground uplift, CO₂ breakthrough at monitoring wells and induced microseismicity, which can be used to validate and improve our models to ensure permanent storage. For instance, the double lobe uplift observed above In Salah KB-502 injection well led to the discovery that a fracture zone could have opened at

depth¹⁵ and the magnitude of the uplift above KB-501 injection well was used to estimate the caprock permeability¹⁶. Rinaldi and Rutqvist¹⁷ calibrated the geometry of the fracture zone at KB-502 by fitting the modeling results with the observed surface uplift data. Additionally, the breakthrough of CO₂ at KB-5 monitoring well, placed 2 km away from the injection well KB-502, permitted estimation of the potential permeability increase of the reservoir¹⁸. This permeability enhancement could be explained by fracture opening due to thermo-hydro-mechanical effects as a result of injection-induced pressure increase and cooling, i.e., as a function of the stress changes¹⁹. As for induced seismicity, despite the significant overpressure and temperature drop induced at In Salah, no felt seismic events have been reported^{20, 21}, though microseismic events have been observed to be correlated with the injection rate²².

Apart from thermo-mechanical effects, the capillary properties of the reservoir, i.e., retention and relative permeability curves, may affect caprock stability because they determine the plume shape, which will influence overpressure distribution. These curves may change during injection due to injection-induced deformation of the porous media²³. Recently, data of the retention and relative permeability curves from the In Salah reservoir have been published²⁴. These curves differ from previous curves used in numerical studies to simulate the In Salah CO₂ storage site (e.g.^{16, 17}). Thus, the sensitivity of these retention and relative permeability curves on the caprock stability should be investigated.

The objective of this work is to analyze the caprock stability at In Salah when injecting cold CO₂. To this end, we use all the available data to model the site as accurately as possible. We first analyze the effect of several retention curves and relative permeability curves on overpressure. Next, we investigate thermo-mechanical effects by comparing CO₂ injection at 50 °C and injection in thermal equilibrium with the storage formation,

i.e., 95 °C, by performing numerical simulations of non-isothermal two-phase flow in deformable porous media. Although the CO₂ injection at In Salah was suspended after about 6 years of operation, we are still modeling and analyzing the caprock stability considering up to 30 years of injection, when the reservoir cooling effects become more substantial, as could be expected at future industrial CO₂ injection sites.

2. METHODS

We consider the injection of cold CO₂ at the In Salah storage site, Algeria. Cold CO₂ injection in a deep confined saline formation induces coupled thermo-hydro-mechanical processes that may affect caprock stability. To solve these couplings, mass conservation of each phase, energy balance and momentum balance may be solved simultaneously in a fully coupled approach. Mass conservation of these two miscible fluids can be written as²⁵,

$$\frac{\partial(\phi S_{\alpha} \rho_{\alpha})}{\partial t} + \nabla \cdot (\rho_{\alpha} \mathbf{q}_{\alpha}) = r_{\alpha}, \quad \alpha = c, w, \quad (1)$$

where ϕ [L³ L⁻³] is porosity, S_{α} [-] is saturation of the α -phase, ρ_{α} [M L⁻³] is density, t [T] is time, \mathbf{q}_{α} [L³ L⁻² T⁻¹] is the volumetric flux, r_{α} [M L⁻³ T⁻¹] is the phase change term (i.e. CO₂ dissolution into water and water evaporation into CO₂) and α is either CO₂ rich phase, c , or aqueous phase, w . When combining the mass balance of the fluids with the mass balance of the solid, a volumetric deformation term appears that couples the flow equation with geomechanics²⁶. For the sake of simplicity we neglect evaporation of water into CO₂, i.e., $r_w = 0$.

Momentum conservation for the fluid phases is given by Darcy's law

$$\mathbf{q}_\alpha = -\frac{kk_{r\alpha}}{\mu_\alpha}(\nabla P_\alpha + \rho_\alpha g \nabla z), \quad \alpha = c, w, \quad (2)$$

where k [L^2] is intrinsic permeability, $k_{r\alpha}$ [-] is the α -phase relative permeability, μ_α

[$M L^{-1} T^{-1}$] its viscosity, P_α [$M L^{-1} T^{-2}$] its pressure and g [$L T^{-2}$] is gravity.

Energy conservation can be expressed as (e.g.,²⁷)

$$\frac{\partial((1-\phi)\rho_s h_s + \phi\rho_w S_w h_w + \phi\rho_c S_c h_c)}{\partial t} - \phi S_c \frac{DP_c}{Dt} + \nabla \cdot (-\lambda \nabla T + \rho_w h_w \mathbf{q}_w + \rho_c h_c \mathbf{q}_c) = 0, \quad (3)$$

where ρ_s [$M L^{-3}$] is solid density, h_α [$L^2 T^{-2}$] is enthalpy of α -phase ($\alpha = c, w, s$; S for solid), λ [$M L T^{-3}$] is thermal conductivity and T [K] is temperature. We assume thermal equilibrium of all phases at every point.

Neglecting inertial terms, the momentum balance of the solid phase is reduced to the equilibrium of stresses

$$\nabla \cdot \boldsymbol{\sigma} + \mathbf{b} = \mathbf{0}, \quad (4)$$

where $\boldsymbol{\sigma}$ [$M L^{-1} T^{-2}$] is the stress tensor and \mathbf{b} [$M L^{-2} T^{-2}$] is the body forces vector.

We assume that the rocks deform elastically. We use linear thermo-elasticity in porous media to include the effect of changes in fluid pressure and temperature on rock strain.

Elastic strain, which depends on total stress, overpressure and temperature, are given by²⁸

$$\boldsymbol{\varepsilon} = \frac{1+\nu}{E} \boldsymbol{\sigma} - \frac{3\nu}{E} \sigma_m \mathbf{I} - \frac{1-2\nu}{E} \Delta P \mathbf{I} - \alpha_T \Delta T \mathbf{I}, \quad (5)$$

where $\boldsymbol{\varepsilon}$ [$L L^{-1}$] is the strain tensor, $\sigma_m = (\sigma_x + \sigma_y + \sigma_z)/3$ [$M L^{-1} T^{-2}$] is the mean stress,

\mathbf{I} [-] is the identity matrix, $P = \max(P_w, P_c)$ is fluid pressure, E [$M L^{-1} T^{-2}$] is the

Young's modulus, ν [-] is Poisson ratio and α_T [K⁻¹] is the thermal expansion

coefficient of the porous medium. The choice of the fluid pressure concept used here, i.e., $P = \max(P_w, P_c)$, does not affect the simulation results because the coupling strength between capillarity and geomechanics is very low²⁹. However, for cases where capillarity is strong, the equivalent pore pressure has to be used²⁹. Here, the sign criterion of geomechanics is adopted, i.e. stress and strain are positive in compression and negative in extension.

To evaluate fracture stability, we conservatively assume that a cohesionless critically oriented fracture could exist at every point, meaning that a standard Mohr-Coulomb failure criterion can be used. Adopting the Mohr-Coulomb failure criterion, the mobilized friction angle can be calculate as

$$\varphi_{mob} = \arctan \left[\frac{\tau}{\sigma_n'} \right], \quad (6)$$

where τ [$M L^{-1} T^{-2}$] is the tangential stress and σ_n' [$M L^{-1} T^{-2}$] is the normal effective stress acting on the cohesionless critically oriented fracture. The mobilized friction angle gives an idea of how close the stress state is to failure conditions. If the mobilized friction angle equals the fracture strength, the fracture undergoes shear slip, which could induce a microseismic event.

Figure 1 schematically represents the geometry and initial and boundary conditions of our model, which is a 2D plane strain representation around one injection well at the In Salah CO₂ storage site. A detailed description of the geological setting of In Salah can be found in Rutqvist²⁰. Table 1 includes the thermo-hydro-mechanical properties of all the rock types considered in the model¹⁷. Table 2 shows the parameters of the retention curve and relative permeability curves used in the sensitivity analysis to test capillary effects on caprock stability. The measured data of the retention curve and relative

permeability curves corresponding to the reservoir at In Salah are taken from Shi et al.²⁴ and the functions used in previous numerical studies are those of Rutqvist et al.¹⁶ and Rinaldi and Rutqvist¹⁷. Additionally, we use for comparison a third set of functions considering a retention curve with the capillary entry pressure used by Rutqvist et al.¹⁶ and the van Genuchten m shape parameter of the adjusted function to the real data, and the relative permeability functions used by Rutqvist et al.¹⁶. Figure 2 shows all these functions, including the adjusted functions to the data given by Shi et al.²⁴.

The initial pressure is hydrostatic and the initial temperature distribution is such that the surface temperature is 30 °C and the temperature at the top of the reservoir is 95 °C². This represents a geothermal gradient of 36 °C/km. The stress state, which is a strike slip stress regime, has been taken from a best estimate of the stress field listed in Morris et al.³⁰. According to this estimate, the vertical stress, σ_v , is lithostatic (with gradient of 24.7 MPa/km), the maximum and the minimum horizontal stresses follow the relationships $\sigma_H = 1.12\sigma_v$ and $\sigma_h = 0.69\sigma_v$, respectively. The minimum horizontal stress coincides with the horizontal well axis and the maximum horizontal stress is perpendicular to the well. As a first step, a steady-state calculation is carried out to ensure consistent initial conditions in equilibrium for the fluid pressure, temperature and stress fields.

We inject 2.33×10^{-3} kg/s/m of CO₂ at 50 °C for 30 years to assess the long-term impact of cold CO₂ on the caprock mechanical stability at In Salah. The injection rate is 1.17×10^{-3} kg/s per meter normal to the model plane. Considering symmetry at the left hand side boundary, it represents 2.33×10^{-3} kg/s per meter of the horizontal well. For a 1.5 km long horizontal well, it represents a total injection rate of 3.5 kg/s, which is about 0.11 million tons per year or 6 million standard cubic feet per day. This injection rate is within the range of injection rates per injection well at In Salah and yields an

overpressure similar to that observed at In Salah. We also simulate a case of CO₂ injection in thermal equilibrium with the storage formation to identify and quantify the induced thermal stresses. To represent the horizontal well, we model half of a 2D cross section perpendicular to the injection well. We assume that the injection well is placed at the bottom of the reservoir. The hydraulic boundary conditions are constant pressure at the outer boundary and no flow at the top and bottom boundaries. The thermal boundary conditions are constant temperature at the top boundary and no flow in the other boundaries. The mechanical boundary conditions are no displacement normal to the bottom, outer and injection well boundaries, and a stress equal to the atmospheric pressure at the top boundary.

The thermo-hydro-mechanical simulations are solved in a fully coupled approach using the finite element numerical code CODE_BRIGTH^{31, 32} extended for CO₂ injection²⁶. The mesh is made of structured quadrilateral elements. Horizontally, the size of the elements is tens of cm close to the injection well and increases progressively up to 1800 m next to the outer boundary. Vertically, the reservoir and tight sands are discretized with 2 m thick elements. The element size progressively grows in the rest of materials up to 400 m toward the upper and lower boundaries. We performed a mesh sensitivity analysis to ensure that results are not affected by further refinements. The 2D model permits using a very fine mesh around the injection well to resolve pressure and temperature gradients near the well and at the reservoir-caprock interface. Such refinement cannot be obtained with 3D models.

3. RESULTS

3.1. CAPILLARY EFFECTS

Figure 3 displays the CO₂ plume shape after 5 years of injection for the three groups of retention curve and relative permeability curves used in this study. The CO₂ plume shape is quite sensitive to changes of these functions. For instance, for a given m shape parameter of the van Genuchten retention curve, a lower entry pressure leads to a lower capillary trapping at the lower part of the reservoir. Therefore, CO₂ tends to float (Figure 3: compare the upper case, high entry pressure, with the lower case, low entry pressure). And for a given entry pressure, a higher van Genuchten m shape parameter yields higher CO₂ saturations and also more buoyancy to CO₂, which tends to concentrate at the top of the reservoir (Figure 3: compare the lower case, high m shape parameter, with the middle case, low m shape parameter).

These differences in the CO₂ plume shape will have an effect on the capillary and dissolution trappings of CO₂ in the post-injection period³³, but the differences have a negligible effect on the injection pressure. Though overpressure differs at the edge of the CO₂ plume because the CO₂-brine interface position varies for different retention and relative permeability curves, the maximum overpressure, which occurs in the vicinity of the injection well, is very similar in all cases. Therefore, caprock stability is practically insensitive to retention and relative permeability curves.

3.2. THERMO-MECHANICAL EFFECTS

The injection of a fluid into a reservoir induces an increase of the horizontal total stresses as a response to overpressure^{20, 26, 34, 35}. If the fluid is colder than the host rock, the thermal contraction causes a thermal stress reduction that is proportional to the temperature difference and the rock stiffness²⁸. Figure 4 shows the total stress changes induced by fluid pressure and temperature changes. The total stress changes propagate

deeper into the basement than into the caprock because of the higher permeability of the basement, which leads to the pressure perturbation advancing further into the basement than into the caprock. The thermal stress is the difference between the two curves, i.e., the one that corresponds to CO₂ injection in thermal equilibrium with the storage formation and the curve that indicates cold CO₂ injection. The largest thermal stress takes place at the bottom of the reservoir because CO₂ is injected there (Figure 4a). The maximum temperature drop coincides with the injection well and dissipates in all directions. Indeed, cooling only occurs within some tens of meters around the injection well (Figure 5). Therefore, thermal stresses are not induced outside of the cooled region (Figure 4b). The small difference in the total stress changes that occurs outside of the cooled region between cold CO₂ injection and CO₂ injection in thermal equilibrium with the storage formation (Figure 4b) is due to the fact that injecting cold CO₂ induces a slightly lower overpressure⁴. This lower overpressure is a consequence of the higher density of cold CO₂, which leads to the displacement of a smaller amount of brine. However, the differences in the total stress changes become larger around the injection well, where cooling takes place (Figure 4a). Unlike isothermal injection, which induces a total stress change very similar in all horizontal directions, cold CO₂ injection induces a larger stress reduction in the minimum horizontal stress direction, along the borehole axis. Therefore, geomechanical stability decreases in this region because (i) the thermal stress reduction displaces the Mohr circle towards the failure envelope and (ii) the larger thermal stress reduction in the minimum horizontal total stress increases the size of the Mohr circle (Figure 6a).

Figure 6 displays the Mohr circles at the bottom of the caprock prior to injection and after 30 years of injection of isothermal and cold CO₂. Since In Salah is under a strike slip stress regime, the maximum and the minimum principal effective stresses are

horizontal, so they are used for defining the Mohr circles, and the vertical effective stress is the intermediate one. When injecting CO₂ in thermal equilibrium with the storage formation, the effective stress changes are uniquely due to overpressure. Since both horizontal total stresses increase similarly, the size of the Mohr circle is maintained. Furthermore, the Mohr circle is displaced towards the yield surface, due to overpressure. However, it is displaced a magnitude smaller than the overpressure because of the increase in the horizontal total stresses. If CO₂ is injected colder than the storage formation, stability is very similar to the isothermal CO₂ injection outside of the cooled region, which is limited to the vicinity of the injection well (Figure 6b). The small differences between the Mohr circles are due to the slightly lower overpressure when injecting cold CO₂. By contrast, the thermal stress reduction that occurs in the cooled region displaces the Mohr circle even more towards the yield surface and increases its size (Figure 6a). Thus, the yield surface may be reached, inducing shear failure and microseismicity. However, tensile failure is far from occurring at the bottom of the caprock because the minimum effective stress remains in compression (Figure 7).

Figure 7, which illustrates the evolution of the maximum and minimum effective stresses, overpressure and temperature change, clearly shows that tensile failure is unlikely to occur at In Salah for a CO₂ injection that is 45 °C colder than the storage formation. Though the thermal stress increases progressively as the lower part of the caprock cools down, the increase rate is so small that the tensile strength may never be reached. The minimum compressive effective stress after 30 years of injection is higher than 5 MPa, but the thermal stress reduction in the minimum compressive effective stress is only of 3 MPa. Figure 7 also shows that the thermal stress in the maximum compressive effective stress is much smaller than in the minimum compressive effective

stress, reducing caprock stability. This reduction in stability is highlighted by the increase in the size of the Mohr circle (recall Figure 6a).

Figure 8 shows the mobilized friction angle (Equation 6) 1 m away from the injection well as a function of depth at several injection times for both CO₂ injection in thermal equilibrium with the storage formation and cold CO₂ injection. The thermal effect is quite concentrated around the injection well for a short injection time, i.e., 1 year (Figure 5a). However, the thermal effect, though still limited to tens of meters around the injection well, propagates further into the caprock and basement for longer injection times (Figure 5c). The high mobilized friction angles of cold CO₂ injection, which indicate that shear failure is likely to occur, are caused by the combined effect of the thermal stress reduction and its anisotropy in the horizontal principal stresses. At the top of the basement, where this anisotropy is the largest (Figure 4a), the highest values of the mobilized friction angle occur. The top of the basement is also the most critical zone when injecting CO₂ in thermal equilibrium with the formation. This is because fluid pressure propagates quickly into the basement because the injection well is immediately above it, but the horizontal total stress increase is much smaller than in the reservoir (Figure 4), which leads to a larger displacement of the stress state towards the failure envelope than in the reservoir.

4. DISCUSSION

Changes in the capillary functions, i.e. retention curve and relative permeability curves, significantly modify the CO₂ plume shape. However, overpressure is almost insensitive to changes of these functions and therefore caprock stability is not affected by capillary effects. These results are in agreement with those of Bao et al.³⁶, who found that the

most relevant factors affecting the geomechanical response to CO₂ injection are reservoir permeability, injection rate and reservoir porosity, but that capillary functions play a minor role.

On the other hand, thermal effects are important and should be considered site specifically, using the most accurate available geomechanical data. Site characterization is key for the success of geologic carbon storage³⁷ and this requires a good hydromechanical characterization³⁸. Rock stiffness and state of stress are essential to determine the maximum sustainable injection pressure³⁹ and the temperature drop with which CO₂ can be injected safely without compromising caprock stability⁴.

Though thermal stress may induce shear slip around the In Salah injection wells (Figure 8), tensile failure is unlikely to occur because the minimum effective stress is in compression throughout the simulated injection (Figure 7). Nevertheless, some uncertainty exists on the actual minimum horizontal stress that could affect this result. Though most of the studies consider similar minimum horizontal stress to the one considered here^{2, 13, 24}, White et al.⁴⁰ estimated that the minimum effective stress was around 24.0 MPa, based on a step rate injectivity test. Such minimum effective stress, which is almost 7 MPa lower than the one used in this study, would probably induce tensile failure. Though our simulation results show that no hydrofracturing is likely to occur, preexisting fractures may open up due to a combination of shearing and the normal effective stress reduction of fractures induced by overpressure and cooling, which may lead to CO₂ migration into the lower portion of the caprock⁴⁰. The absence of tensile stresses is in disagreement with the results of Preisig and Prevost¹⁰ and Gor et al.¹³, who predicted tensile stresses in the lower part of the caprock after several years of cold CO₂ injection. This difference cannot be due to the numerical scheme, because in their simulations and in our own simulations, a fully coupled numerical code has been

used. It can neither be due to the pore pressure definition, because the geomechanical results are not affected by the pore pressure definition due to the very low capillarity of this problem²⁹. However, the difference in the stress changes may be due to the fact that they placed the injection well in the middle of the reservoir and that they did not include the basement in their model, through which fluid penetrates further than into the caprock due to its higher permeability.

The increase of shear slip potential that occurs due to thermal stresses in this model also differs from the results of Vilarrasa et al.⁴, who found that cold CO₂ injection in a 100 m thick reservoir does not worsen caprock stability in a reverse faulting stress regime and even improves caprock stability in a normal faulting stress regime. The reasons for this difference in caprock stability are multifold: the state of stress, the thickness of the reservoir and the orientation of the injection well. First, the stress state considered in this study is different from those considered by Vilarrasa et al.⁴. While the maximum and the minimum effective stresses coincide with the vertical and horizontal direction in a normal and a reverse faulting stress regimes, they are contained within the horizontal plane in a strike slip stress regime. This is relevant because the changes in effective stresses are much different between the vertical and horizontal direction than between the two horizontal directions. In a normal faulting stress regime, the Mohr circle shrinks at the bottom of the caprock due to an increase in the total horizontal stresses induced by thermal effects and therefore, the caprock tightens. In a reverse faulting stress regime, the Mohr circle expands slightly, but due to the high confining pressure, the decrease in stability compared to the isothermal case is small. However, in a strike slip stress regime, the Mohr circle is displaced to the left due to the thermal stresses reduction and also increases in size due to the anisotropy in the thermal stresses in the horizontal direction (Figure 6a). Therefore, caprock stability decreases. Another factor

that affects caprock stability is the reservoir thickness. The reservoir in the study of Vilarrasa et al.⁴ is very thick (100 m), leading to a significant reduction of the vertical total stress within the reservoir. To satisfy stress balance, stress redistribution around the cooled volume occurs, causing the horizontal total stresses to increase at the bottom of the reservoir. However, the reservoir thickness at In Salah is much thinner (20 m) and therefore, the vertical total stress reduction takes place in a much smaller volume. Note that outside of the cooled region, the vertical total stress is maintained constant (Figure 4b). Therefore, the stress redistribution is smaller, leading to a lower increase of the horizontal total stresses at the bottom of the caprock. The effect of the reservoir thickness on normal fault reactivation was also recently studied by Rinaldi et al.⁴¹. Their results show that, for a given injection rate, if the pressurization reaches the critical value to reactivate the fault, the thicker the reservoir, the larger the seismic event magnitude. Finally, the orientation of the injection well affects caprock stability⁴². When injecting CO₂ through a horizontal well, thermal stresses are higher at the injection well, which is usually placed at the bottom of the reservoir. This may seem beneficial because the caprock is less affected by the thermal stress reduction. On the other hand, if CO₂ is injected through a vertical well, the whole reservoir is cooled and the vertical stress reduction affects a larger volume of rock, which may enhance the increase in the horizontal total stress and therefore, tighten the caprock. However, these thermal effects due to reservoir thickness and orientation of the well need further investigation.

This and previous studies^{4, 14} reveal that thermal stresses can be estimated and controlled. Therefore, thermal stresses should not be feared, we just need to anticipate their potential effects, which can be positive in some cases⁴. Since CO₂ will likely reach the storage formation at a colder temperature than that of the host rock¹⁴, the analysis of thermo-mechanical effects associated with CO₂ injection sites will be required. Though

temperature changes will occur only in the vicinity of the injection well (Figure 5), it is important to consider them in order to avoid damage to the caprock that could lead to CO₂ leakage. Apart from thermo-mechanical effects, the affection that overpressure has on faults located far away from the injection well should also be studied. Such faults could be reactivated, inducing a seismic event^{41, 43-46}. Nevertheless, at the In Salah CO₂ storage site, our analysis shows that the mobilized friction angle prior to injection is relatively low, around 25 ° (Figure 8) and therefore, there is probably wide margin before fractures and faults are reactivated at a significant rate. Note that far away from the injection well, CO₂ will have already thermally equilibrated with the storage formation (Figure 5) and therefore, no thermal stresses will be induced. Figure 8 shows that the mobilized friction angle within the reservoir next to the injection well for an isothermal injection, despite the substantial overpressure, is lower than 30 °, which is frequently considered as the strength of fractures and faults⁴⁷. Thus, further away from the injection well, i.e., outside of the cooled region and where overpressure is significantly smaller, the mobilized friction angle will be smaller and therefore fractures and faults are unlikely to be reactivated. This is in agreement with simulation results presented by Rutqvist²⁰, which showed that the highest potential for induced microseismicity occurs close to the injection well. On the other hand, the analysis by Morris et al.³⁰ indicated that minor faults within the reservoir and away from the injection wells could be reactivated and thereby become more hydraulic conducting. However, the analytical analysis Morris et al.³⁰ is based on the initial (pre-injection) stress state, injection-induced changes in pressure and effective stress, without consideration of injection induced changes in the total stress field. As pointed out in Rutqvist²⁰, no felt seismic event have been reported from the site indicating that large portions of those minor fault have not been reactivated in shear. Though microseismic

events have been measured at In Salah and slip can also occur aseismically⁴⁸, no evidence exists that CO₂ has leaked out of the storage formation⁴⁹. Nevertheless, reservoir permeability may have increased because of these microseismicity or aseismic slip¹⁹.

Finally, we show that for the best estimated stress field considered in this study, and for the injection pressure and temperature measured in the field, the potential for shear activation of fractures in the reservoir and lower part of the caprock would increase after a few years of injection. The analysis (Figure 8) shows that this may only affect the lowest tens of meters of the 900 m thick caprock and would therefore not jeopardize the confinement of the injected CO₂. The shear failure in this lower part of the caprock could result in shear slip along pre-existing fractures that could give rise to unfelt microseismic events. Indeed, such microseismic events have been monitored at the site, in periods of higher injection rate²². Our analysis indicates that thermal effects may have been one important factor of triggering at least some of those events around the injection wells. Such shear activation of existing fractures in the reservoir and in the lower caprock may be beneficial for the CO₂ storage operation as this could lead to increased permeability and accessible porosity that in turn would have a positive effect on injectivity and available storage volume. Nevertheless, detailed studies should be performed site specifically to determine the maximum temperature drop that the caprock can undergo without inducing fracture propagation that could cross the whole caprock⁵⁰.

5. CONCLUSIONS

We analyze thermal and capillary effects on the caprock mechanical stability at the In Salah CO₂ storage site, Algeria. Capillary effects are not relevant on the caprock stability because the induced overpressure is almost insensitive to changes in the retention and relative permeability curves. However, thermal effects have a significant effect on caprock stability around the injection well for the geological setting considered in this study, which is based on In Salah. For injection through a horizontal well, the injection-induced thermal stresses are anisotropic in the horizontal plane, which, apart from displacing the Mohr circle to the left, can cause an increase in the Mohr circle size. The Mohr circle will increase in size if the horizontal well is oriented parallel with the minimum compressive stress, which is a common practice and also the case at In Salah. Our analysis shows that the thermo-mechanical response to cold CO₂ injection and its effect on caprock stability strongly depends on the local stress regime, i.e., normal faulting, reverse faulting or strike slip, which highlights the necessity of site specific analysis.

At In Salah, injection-induced thermal stresses may have caused shear slip of pre-existing fractures in the region affected by cooling, which concentrates in the vicinity of the injection well. In the case that this shear slip has occurred, it has been restricted to small shear displacements on small fractures that may be the source of (unfelt) microseismic events that were detected during injection at the site. However, tensile failure induced by thermal stress is unlikely to occur at the bottom of the caprock because the analysis shows that the minimum compressive effective stress remains in compression. Thus, although excessive cooling should be limited in order to reduce the effect on caprock stability, it appears that the cooling at In Salah has been beneficial to the injection operation with potential increase in accessible porosity that could provide additional storage volume in the lowest part of the caprock. Indeed, the analysis shows

that only the reservoir and the lowest tens of meters of the 900 m thick caprock were affected by the cooling effects, which would thus not jeopardize the overall sealing capacity of the caprock.

Overall, thermo-mechanical effects should be analyzed before CO₂ is injected at any site in order to determine the temperature drop that should not be exceeded to avoid damage to the caprock that could lead to CO₂ leakage. To perform this analysis, a proper geomechanical site characterization, which measures the stress state and rock stiffness, is required. This analysis prior to injection should be followed by a monitoring system controlling overpressure, temperature changes and microseismicity in order to ensure that injection evolves as expected and to adapt the injection parameters as more information is collected and the knowledge of the site is improved.

ACKNOWLEDGMENTS

This work was funded by the Assistant Secretary for Fossil Energy, Office of Natural Gas and Petroleum Technology, through the National Energy Technology Laboratory under U.S. Department of Energy Contract No. DE-AC02-05CH11231. Review comments on the initial manuscript by Lykke Gemmer, Statoil, are greatly appreciated. The authors would like to thank the In Salah JIP and their partners BP, Statoil, and Sonatrach for providing field data and technical input over the past 8 years as well as for financial support during LBNL's participation in the In Salah JIP, 2011 – 2013.

REFERENCES

1. Paterson L, Lu M, Connell LD and Ennis-King J, Numerical modeling of pressure and temperature profiles including phase transitions in carbon dioxide wells. *SPE Annual Technical Conference and Exhibition*, Denver, 21-24 September (2008).
2. Bissell RC, Vasco DW, Atbi M, Hamdani M, Okwelegbe M and Goldwater MH, A full field simulation of the In Salah gas production and CO₂ storage project using a coupled geo-mechanical and thermal fluid flow simulator. *Energy Procedia* **4**:3290–3297 (2011).
3. Kim S and Hosseini SA, Above-zone pressure monitoring and geomechanical analyses for a field-scale CO₂ injection project in Cranfield, MS. *Greenhouse Gases: Science and Technology* **4**(1):81-98 (2014).
4. Vilarrasa V, Silva O, Carrera J and Olivella S, Liquid CO₂ injection for geological storage in deep saline aquifers. *International Journal of Greenhouse Gas Control* **14**:84–96 (2013).
5. Ghassemi A, Tarasovs S and Cheng AH-D, A 3-D study of the effects of thermomechanical loads on fracture slip in enhanced geothermal reservoirs. *International Journal of Rock Mechanics and Mining Sciences*, **44**:1132-1148 (2007).
6. Koh J, Roshan H and Rahman SS, A numerical study on the long term thermo-poroelastic effects of cold water injection into naturally fractured geothermalreservoirs. *Computers & Geotechnics* **38**:669–682 (2011).

7. de Simone S, Vilarrasa V, Carrera J, Alcolea A and Meier P, Thermal coupling may control mechanical stability of geothermal reservoirs during cold water injection. *Journal of Physics and Chemistry of the Earth* **64**:117-126 (2013).
8. Rutqvist J, Dobson PF, Garcia J, Hartline C, Jeanne P, Oldenburg CM, Vasco DW and Walters M, The Northwest Geysers EGS Demonstration Project, California: pre-stimulation modeling and interpretation of the stimulation. *Mathematical Geosciences* <http://dx.doi.org/10.1007/s11004-013-9493-9500> (2013).
9. Rinaldi AP, Rutqvist J, Sonnenthal EL and Cladouhos TT, Coupled THM Modeling of Hydroshearing Stimulation in Tight Fractured Volcanic Rock. *Transport in Porous Media* Online First (2014).
10. Preisig M and Prévost JH, Coupled multi-phase thermo-poromechanical effects. Case study: CO₂ injection at In Salah, Algeria. *International Journal of Greenhouse Gas Control* **5**(4):1055–1064 (2011).
11. Goodarzi S, Settari A and Keith D, Geomechanical modeling for CO₂ storage in Nisku aquifer in Wabamun lake area in Canada. *International Journal of Greenhouse Gas Control* **10**:113–122 (2012).
12. Fang Y, Nguyen BN, Carroll K, Xu Z, Yabusaki SB, Scheibe TD and Bonneville A, Development of a coupled thermo-hydro-mechanical model in discontinuous media for carbon sequestration. *International Journal of Rock Mechanics and Mining Sciences* **62**:138–147 (2013).
13. Gor YG, Elliot TR and Prévost JH, Effects of thermal stresses on caprock integrity during CO₂ storage. *International Journal of Greenhouse Gas Control* **12**:300–309 (2013).
14. Vilarrasa V, Olivella S, Carrera J and Rutqvist J, Long term impacts of cold CO₂ injection on the caprock integrity. *International Journal of Greenhouse Gas Control* **24**:1-13 (2014).
15. Vasco DW, Ferretti A and Novali F, Reservoir monitoring and characterization using satellite geodetic data: interferometric synthetic aperture radar observations from the Krechba field, Algeria. *Geophysics* **73**(6), WA113–WA122 (2008).
16. Rutqvist J, Vasco DW and Myer L, Coupled reservoir-geomechanical analysis of CO₂ injection and ground deformations at In Salah, Algeria. *International Journal of Greenhouse Gas Control* **4**(2):225–230 (2010).
17. Rinaldi AP and Rutqvist J, Modeling of deep fracture zone opening and transient ground surface uplift at KB-502 CO₂ injection well, In Salah, Algeria. *International Journal of Greenhouse Gas Control* **12**:155–167 (2013).

18. Iding M and Ringrose P, Evaluating the impact of fractures on the performance of the In Salah CO₂ storage site. *International Journal of Greenhouse Gas Control* **4**:242-248 (2010).
19. Rinaldi AP, Rutqvist J, Finsterle S and Liu HH, Forward and inverse modeling of ground surface uplift at In Salah, Algeria. *Proceedings of the 48th US Rock Mechanics – Geomechanics Symposium*, Minneapolis, Minnesota, June 1-4 (2014).
20. Rutqvist J, The geomechanics of CO₂ storage in deep sedimentary formations. *International Journal of Geotechnical and Geological Engineering* **30**:525–551 (2012).
21. IEAGHG, Induced seismicity and its implications for CO₂ storage risk. 2013/09, June (2013).
22. Oye V, Aker E, Daley TM, Kühn D, Bohlooli B and Korneev V, Microseismic monitoring and interpretation of injection data from the In Salah CO₂ storage site (Krechba), Algeria. *Energy Procedia* **37**:4191–4198 (2013).
23. Liu H-H, Wei M-Y and Rutqvist J, Normal-stress dependence of fracture hydraulic properties including two-phase flow properties. *Hydrogeology Journal* **21**:371-382 (2013).
24. Shi J-Q, Sinayuc C, Durucan S and Korre A, Assessment of carbon dioxide plume behavior within the storage reservoir and the lower caprock around the KB-502 injection well at In Salah. *International Journal of Greenhouse Gas Control* **7**:115-126 (2012).
25. Bear J (ed.), *Dynamics of fluids in porous media*. Elsevier, New York (1972).
26. Vilarrasa V, Bolster D, Olivella S and Carrera J, Coupled hydromechanical modeling of CO₂ sequestration in deep saline aquifers. *International Journal of Greenhouse Gas Control* **4**(6):910-919 (2010).
27. Nield DA and Bejan A, *Convection in porous media*. Springer, New York (2006).
28. Segall P and Fitzgerald SD, A note on induced stress changes in hydrocarbon and geothermal reservoirs. *Tectonophysics* **289**:117-128 (1998).
29. Kim J, Tchelepi HA and Juanes R, Rigorous coupling of geomechanics and multiphase flow with strong capillarity. *SPE Journal* **18**(06):1-123 (2013).
30. Morris JP, Hao Y, Foxall W and McNab W, A study of injection-induced mechanical deformation at the In Salah CO₂ storage project. *International Journal of Greenhouse Gas Control* **5**(2):270-280 (2011).
31. Olivella S, Carrera J, Gens A and Alonso EE, Non-isothermal multiphase flow of brine and gas through saline media. *Transport In Porous Media* **15**:271–293 (1994).

32. Olivella S, Gens A, Carrera J and Alonso EE, Numerical formulation for a simulator (CODE_BRIGHT) for the coupled analysis of saline media. *Eng. Computations* **13**:87–112 (1996).
33. MacMinn CW and Juanes R, Post-injection spreading and trapping of CO₂ in saline aquifers: impact of the plume shape at the end of injection. *Computational Geoscience* **13**:483-491 (2009).
34. Streit JE and Hillis RR, Estimating fault stability and sustainable fluid pressures for underground storage of CO₂ in porous rock. *Energy* **29**:1445-1456 (2004).
35. Jaeger JC, Cook NGW and Zimmerman RW (ed.), *Fundamentals of rock mechanics*. 4th Edition, Wiley-Blackwell, Oxford (2007).
36. Bao J, Hou Z, Fang Y, Ren H and Lin G, Uncertainty quantification for evaluating impacts of caprock and reservoir properties on pressure buildup and ground surface displacement during geological CO₂ sequestration. *Greenhouse Gases: Science and Technology* **3**(5):338-358 (2013).
37. Juanes R, Hager BH and Herzog HJ, No geologic evidence that seismicity causes fault leakage that would render large-scale carbon capture and storage unsuccessful. *Proceedings of the National Academy of Sciences* **109**(52):E3623-E3623 (2012).
38. Vilarrasa V, Carrera J and Olivella S, Hydromechanical characterization of CO₂ injection sites. *International Journal of Greenhouse Gas Control* **19**:665-677 (2013).
39. Rutqvist J, Birkholzer JT, Cappa F and Tsang C-F, Estimating maximum sustainable injection pressure during geological sequestration of CO₂ using coupled fluid flow and geomechanical fault-slip analysis. *Energy Conversion Management* **48**:1798–1807 (2007).
40. White JA, Chiaramonte L, Ezzedine S, Foxall W, Hao Y, Ramirez A and McNab W, Geomechanical behavior of the reservoir and caprock system at the In Salah CO₂ storage project. *Proceedings of the National Academy of Sciences*, doi:10.1073/pnas.1316465111 (2014).
41. Rinaldi AP, Jeanne P, Rutqvist J, Cappa F and Guglielmi Y, Effects of fault-zone architecture on earthquake magnitude and gas leakage related to CO₂ injection in a multi-layered sedimentary system. *Greenhouse Gases: Science and Technology* **4**:99-120 (2014).
42. Vilarrasa V, Impact of CO₂ injection through horizontal and vertical wells on the caprock mechanical stability. *International Journal of Rock Mechanics and Mining Sciences* **66**:151-159 (2014).

43. Cappa F and Rutqvist J, Impact of CO₂ geological sequestration on the nucleation of earthquakes. *Geophysical Research Letters* **38**, L17313, doi: 10.1029/2011GL048487 (2011).
44. Mazzoldi A, Rinaldi AP, Borgia A and Rutqvist J, Induced seismicity within geologic carbon sequestration projects: Maximum earthquake magnitude and leakage potential. *International Journal of Greenhouse Gas Control* **10**:434–442 (2012).
45. Rinaldi AP, Rutqvist J and Cappa F, Geomechanical effects on CO₂ leakage through fault zones during large-scale underground injection. *International Journal of Greenhouse and Gas Control* **20**:117-131 (2014).
46. Jha B and Juanes R, Coupled multiphase flow and poromechanics: A computational model of pore pressure effects on fault slip and earthquake triggering. *Water Resources Research* **50**(5):3776-3808 (2014).
47. Byerlee JD, Friction of rocks. *Pure Applied Geophysics* **116**:615-629 (1978).48. Cornet FH, Helm J, Poitrenaud H and Etchecopar A, Seismic and aseismic slips induced by large-scale fluid injections. *Pure and Applied Geophysics* **150**:563-583 (1997).
48. Cornet FH, Helm J, Poitrenaud H and Etchecopar A, Seismic and aseismic slips induced by large-scale fluid injections. *Pure and Applied Geophysics* **150**:563-583 (1997).
49. Stork AL, Verdon JP and Kendall JM, The microseismic response at the In Salah Carbon Capture and Storage (CCS) site. *International Journal of Greenhouse Gas Control* **32**:159-171 (2015).
50. Gor GY, Stone HA and Prévost JH, Fracture propagation driven by fluid outflow from a low-permeability aquifer. *Transport in Porous Media* **100**(1):69-82 (2013).

TABLES

Table 1. Properties of the rocks considered in the model of In Salah, Algeria.

Property	Reservoir	Tight sands	Lower caprock	Caprock	Shallow aquifer	Basement
Permeability, k (m ²)	$1.3 \cdot 10^{-14}$	10^{-21}	10^{-21}	10^{-21}	10^{-12}	10^{-19}
Relative water permeability, k_{rw} (-)	$S_w^{5.25}$	S_w^6	S_w^6	S_w^6	S_w^3	S_w^6
Relative CO ₂ permeability, k_{rc} (-)	$S_c^{3.5}$	S_c^6	S_c^6	S_c^6	S_c^3	S_c^6
Gas entry pressure, P_0 (MPa)	0.1	0.621	0.621	0.621	0.0199	0.621
van Genuchten shape parameter m (-)	0.7	0.457	0.457	0.457	0.457	0.457
Residual liquid saturation, S_{rw} (-)	0.31	0.3	0.3	0.3	0.3	0.3
Porosity (-)	0.17	0.01	0.01	0.01	0.1	0.01
Young's modulus, E (GPa)	10	20	2	5	3	15

Poisson ratio, ν (-)	0.2	0.25	0.3	0.3	0.25	0.3
Thermal conductivity, λ (W/m/K)	2.4	1.5	1.5	1.5	2.4	1.5
Solid specific heat capacity, c_p (J/kg/K)	890	890	890	890	890	890
Bulk thermal expansion coefficient, α_T ($^{\circ}\text{C}^{-1}$)	10^{-5}	10^{-5}	10^{-5}	10^{-5}	10^{-5}	10^{-5}

Table 2. Properties of the retention curve and relative permeability curves used in the sensitivity analysis of the capillary effects on caprock stability.

Property	Adjusted functions	Previous functions	Additional functions
Relative water permeability, k_{rw} (-)	$S_w^{5.25}$	S_w^3	S_w^3
Relative CO ₂ permeability, k_{rc} (-)	$S_c^{3.5}$	S_c^3	S_c^3
Gas entry pressure, p_0 (MPa)	0.1	0.019	0.019
van Genuchten shape parameter m (-)	0.7	0.457	0.7
Residual liquid saturation, S_{rw} (-)	0.31	0.3	0.3

FIGURES

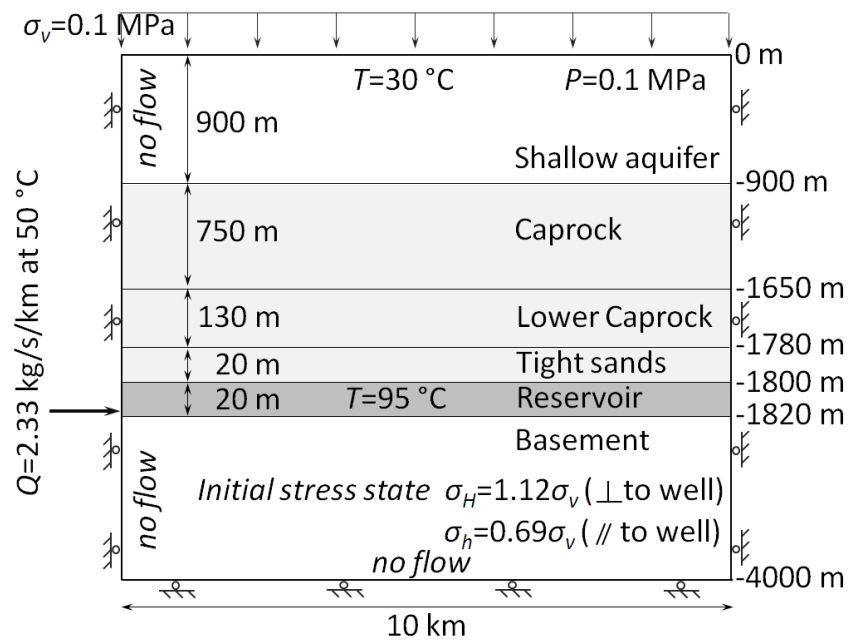


Figure 1. Schematic representation (not to scale) of the model geometry and initial and boundary conditions. The model is based on the In Salah, Algeria, CO₂ storage site.

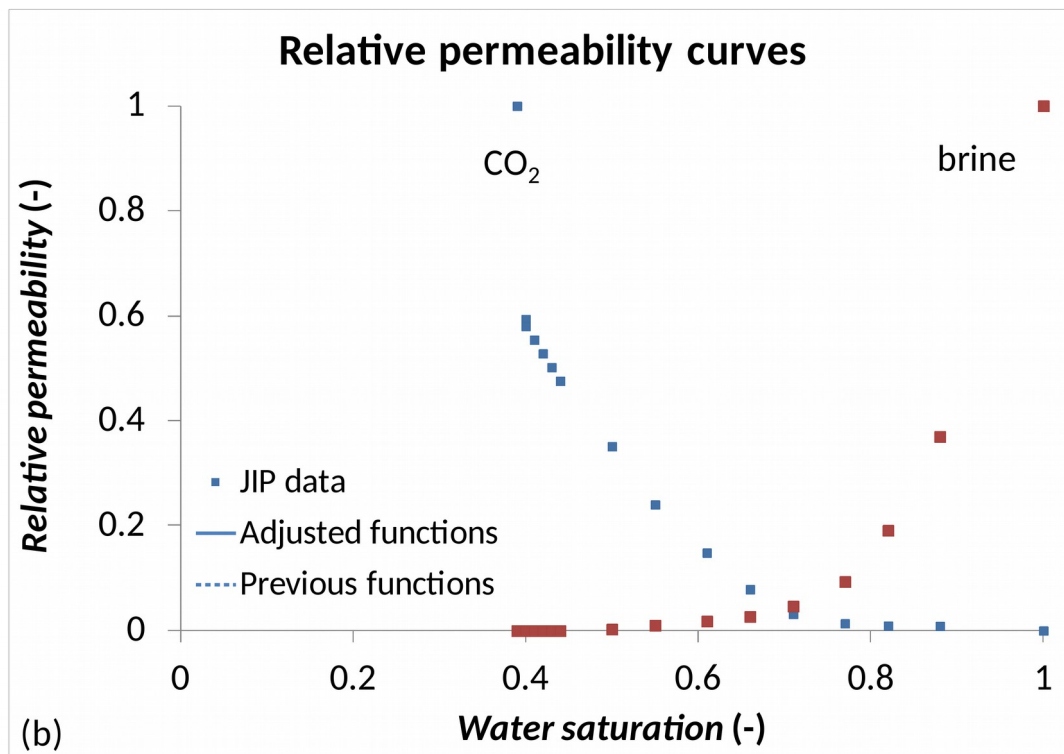
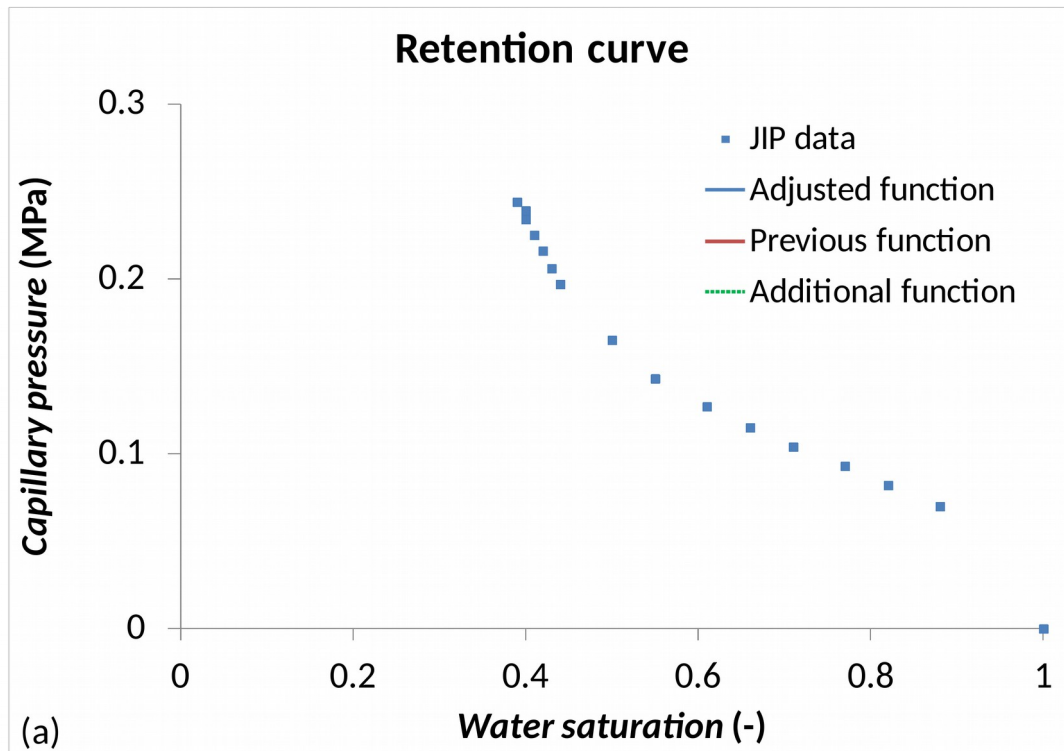


Figure 2. Capillary functions used in the sensitivity analysis. (a) Retention curve (blue line) adjusted to the capillary pressure data of In Salah (blue squares), retention curve used in previous numerical studies of In Salah (red line) and a third retention curve used for comparison (green dashed line, see text for details). (b) Relative permeability curves (continuous lines) adjusted to the data of In Salah (squares) and the relative

permeability curves used in previous numerical studies of In Salah (dashed lines; also used for the third case).

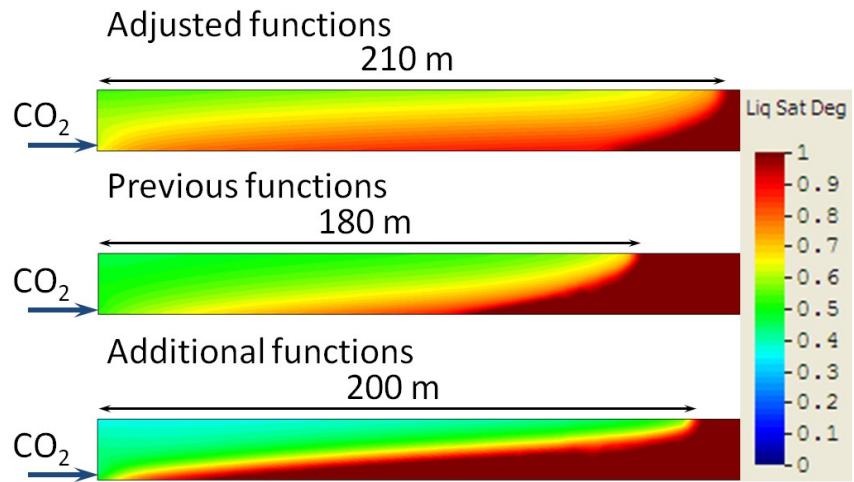


Figure 3. CO₂ plume shape within the reservoir after 5 years of injection for the three cases considered in this sensitivity study.

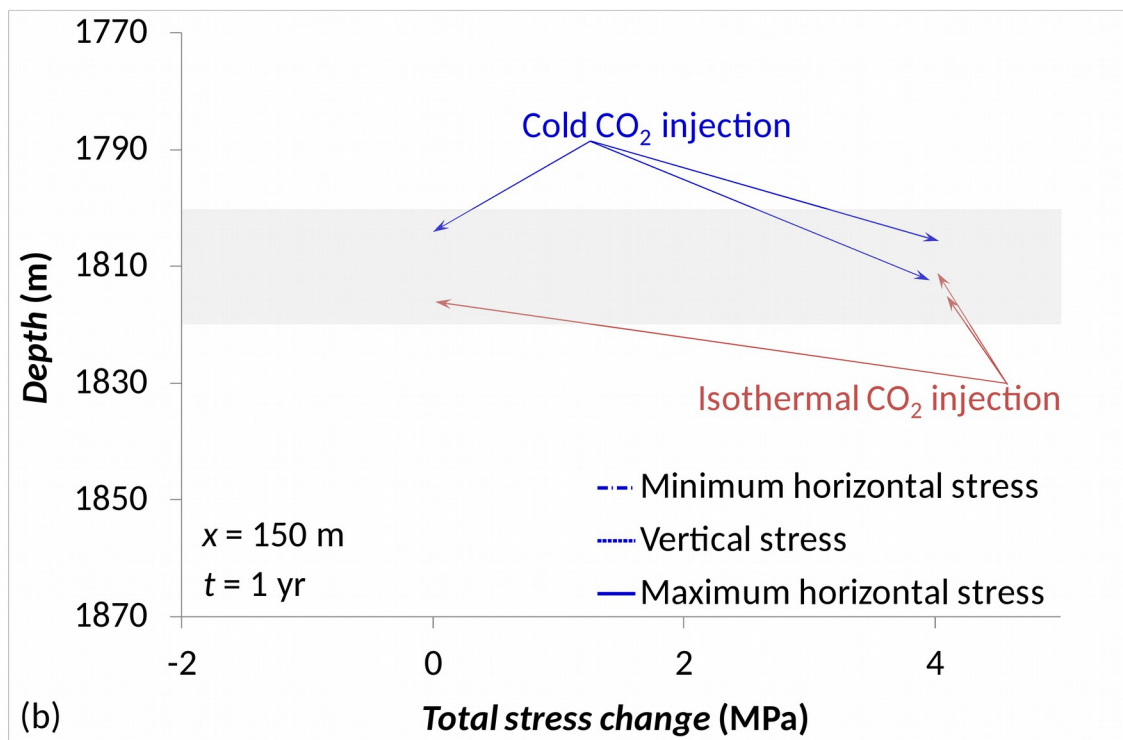
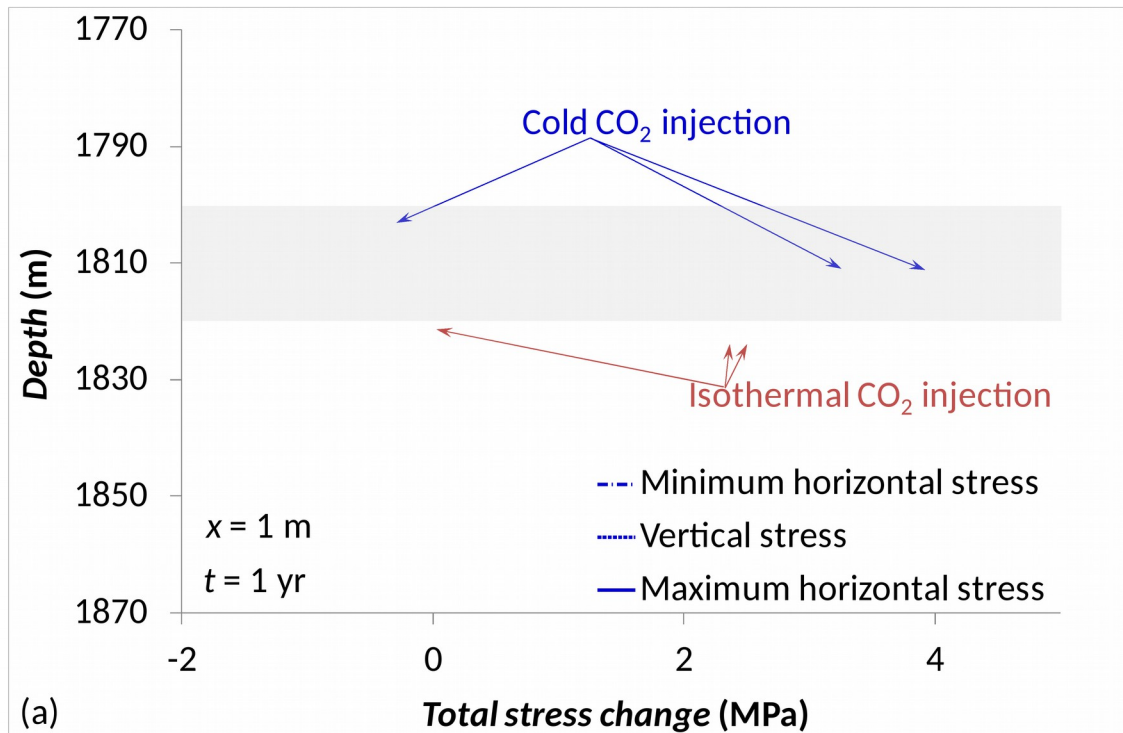


Figure 4. Total stress changes as a function of depth after 1 year of injecting CO_2 in thermal equilibrium with the formation and CO_2 at 50°C (45°C colder than the storage formation), (a) 1 m away from the injection well and (b) 150 m away from the injection well, where cooling does not take place.

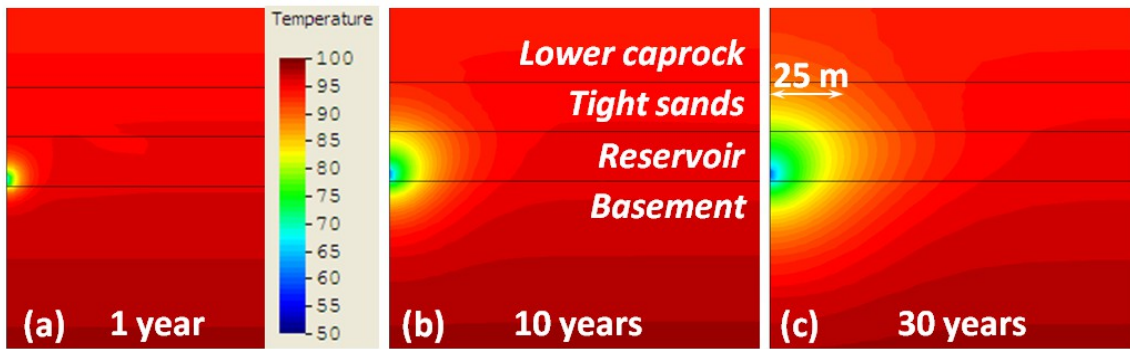


Figure 5. Temperature distribution around the injection well after (a) 1, (b) 10 and (c) 30 years of CO₂ injection at 50 °C. Cooling is limited to tens of meters around the injection well. The cooling front advances much behind than the desaturation front, which reaches 1200 m after 30 years of injection.

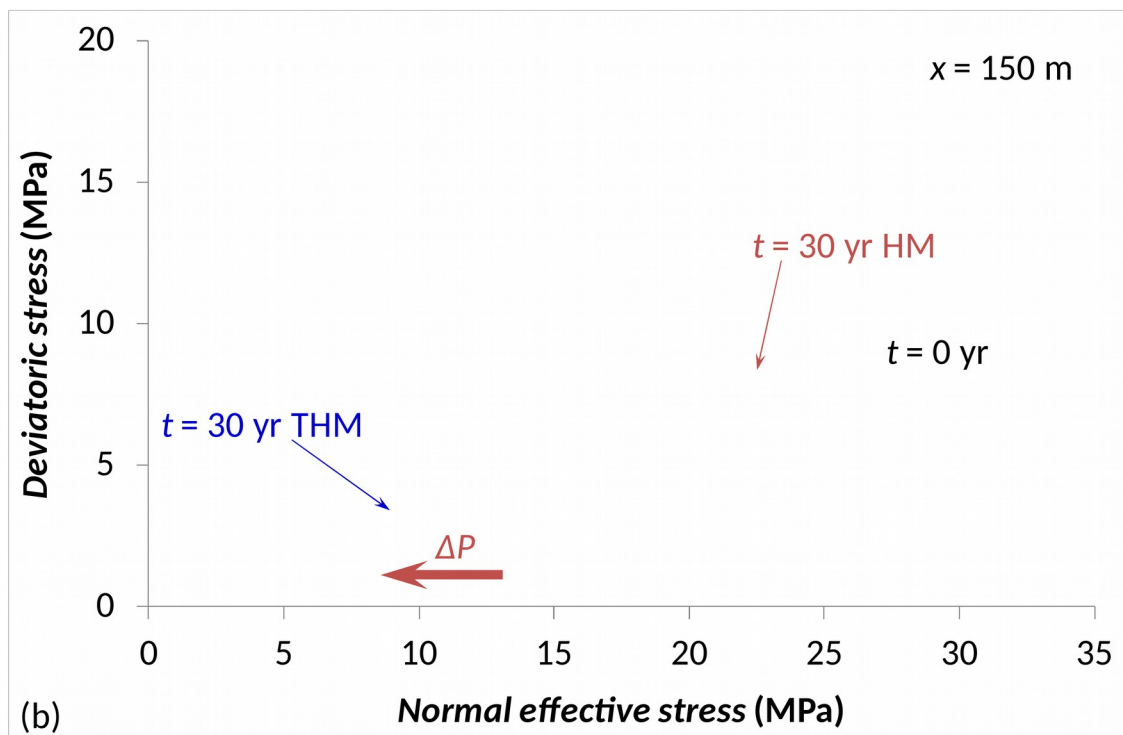
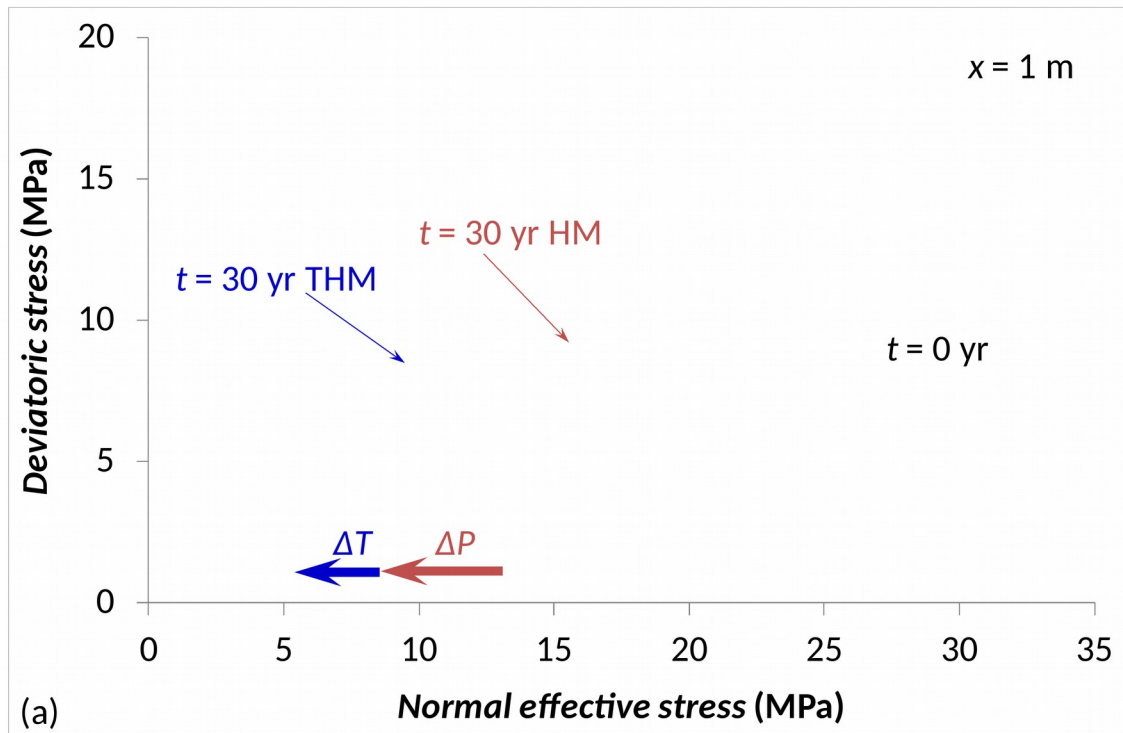


Figure 6. Mohr circles of the bottom of the caprock, (a) 1 m away from the injection well and (b) 150 m away from the injection well, prior to injection and after 30 years of injection of CO_2 in thermal equilibrium with the formation (HM) and cold CO_2 (THM). The red arrow indicates the effect induced by overpressure, which also includes the increase in the horizontal total stresses, and the blue arrow indicates the effect of the temperature reduction, which also incorporates the anisotropy of the thermal stress in

the horizontal directions that causes the increase in size of the Mohr circle. Cooling does not occur 150 m away from the injection well and therefore, no thermal stresses are induced.

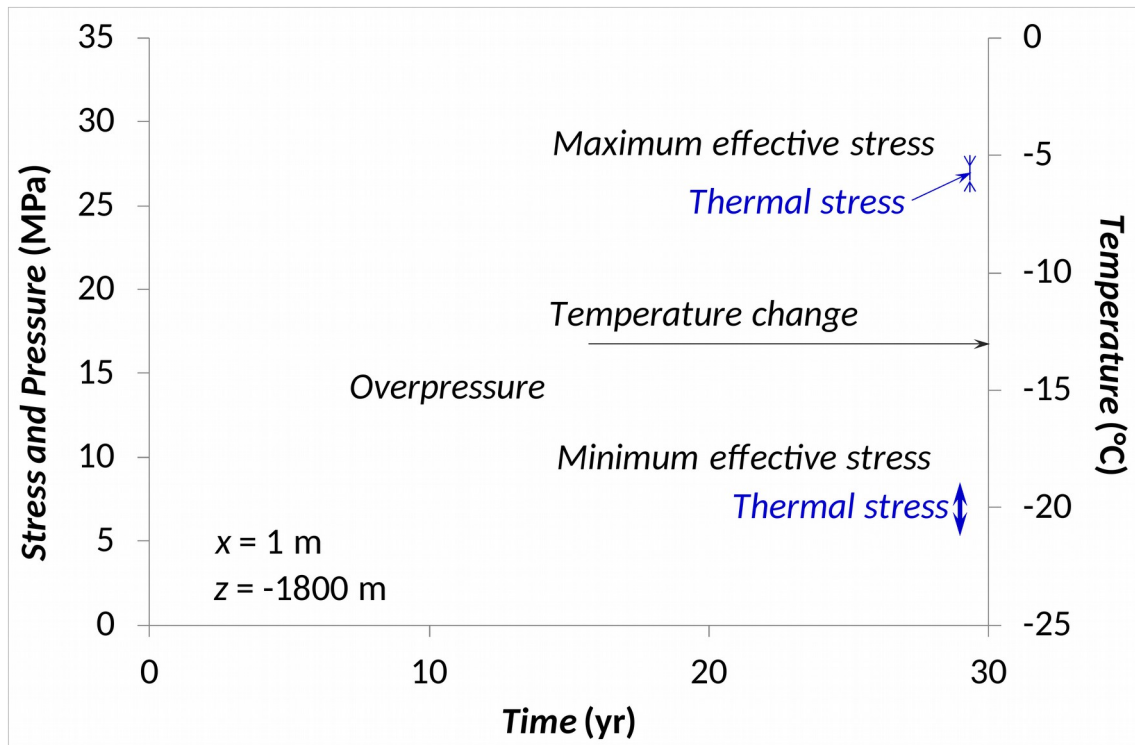


Figure 7. Evolution of the maximum and minimum effective stresses, overpressure and temperature change at the bottom of the caprock above the injection well. The red lines of the maximum and minimum effective stresses represent CO₂ injection in thermal equilibrium with the storage formation and the blue lines indicate cold CO₂ injection. The thermal stress is the difference between these two lines.

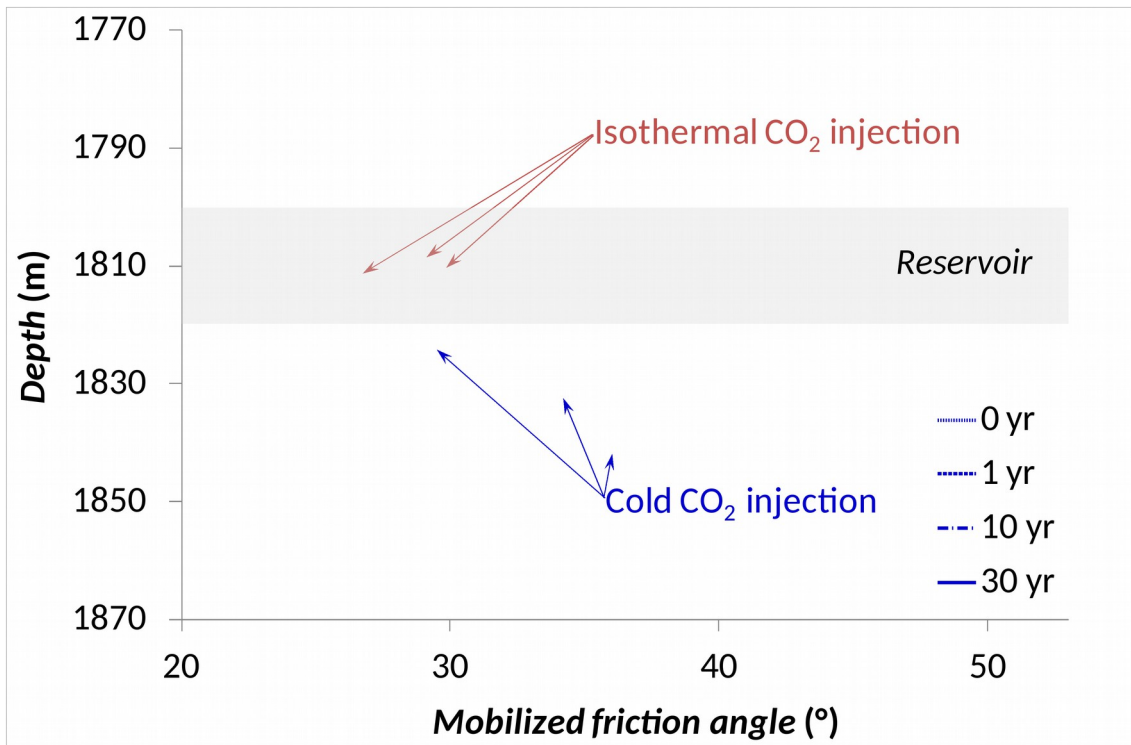


Figure 8. Mobilized friction angle as a function of depth at 0, 1, 10 and 30 years of injecting CO₂ in thermal equilibrium with the storage formation and cold CO₂, computed 1 m away from the injection well.